# Small-angle neutron scattering of ionic perfluoropolyether micellar solutions: Role of counterions and temperature.

# Small-Angle Neutron Scattering of Ionic Perfluoropolyether Micellar Solutions: Role of Counterions and Temperature

**C. M. C. Gambi,*,†,‡ R. Giordano,§ A. Chittofrati,|| R. Pieri,|| P. Baglioni,⊥ and J. Teixeira▽**

*Department of Physics, University of Florence and I.N.F.M., v. G. Sansone 1, 50019 Sesto Fiorentino, Firenze, Italy, Department of Physics, University of Messina and I.N.F.M., Salita Sperone 31, 98010 S. Agata, Messina, Italy, Solvay Solexis, Research & Technology, Physical Chemistry of Interfaces, viale Lombardia 20, 20021 Bollate, Milano, Italy, Department of Chemistry, University of Florence and C.S.G.I., v. della Lastruccia 3, 50019 Sesto Fiorentino, Firenze, Italy, Laboratoire Léon Brillouin, CEA-CNRS Saclay, 91191 Gif sur Yvette Cédex, France, and I.N.F.M. CRS-SOFT, Università Roma "La Sapienza", P.le A. Moro 2, 00185 Rome, Italy*

*Received: August 24, 2004; In Final Form: February 1, 2005*

This paper reports a small-angle neutron scattering (SANS) characterization of perfluoropolyether (PFPE) aqueous micellar solutions with lithium, sodium, cesium and diethanol ammonium salts obtained from a chlorine terminated carboxylic acid and with two perfluoroisopropoxy units in the tail ($n_2$). The counterion and temperature effects on the micelle formation and micellar growth extend our previous work on ammonium and potassium salts $n_2$ micellar solutions. Lithium, sodium, cesium and diethanol ammonium salts are studied at 0.1 and 0.2 M surfactant concentration in the temperature interval 28−67 °C. SANS spectra have been analyzed by a two-shell model for the micellar form factor and a screened Coulombic plus steric repulsion potential for the structure factor in the frame of the mean spherical approximation of a multicomponent system reduced to a generalized one component macroions system (GOCM). At 28 °C, for all the salts, the micelles are ellipsoidal with an axial ratio that increases from 1.6 to 4.2 as the counterion volume increases. The micellar core short axis is 13 Å and the shell thickness 4.0 Å for the alkali micelles, and 14 and 5.1 Å for the diethanol ammonium micelles. Therefore, the core short axis mainly depends on the surfactant tail length and the shell thickness on the carboxylate polar head. The bulky diethanol ammonium counterion solely influences the shell thickness. Micellar charge and average aggregation number depend on concentration, temperature and counterion. At 28 °C, the fractional ionization decreases vs the counterion volume (or molecular weight) increase at constant concentration for both $C = 0.1$ M and $C = 0.2$ M. The increase of the counterion volume leads also to more ellipsoidal shapes. At $C = 0.2$ M, at 67 °C, for sodium and cesium micelles the axial ratio changes significantly, leading to spherical micelles with a core radius of 15 Å, lower average aggregation number, and larger fractional ionization.

## Introduction

We have recently studied, by small-angle neutron scattering (SANS), perfluoropolyether (PFPE) micellar solutions in water. They can be obtained by ammonium or potassium salts of a carboxyl acid ($Cl(C_3F_6O)_2CF_2COOH$) terminated with chlorine and with two perfluoroisopropoxy units in the tail ($n_2$).[1,2] Although the study on aqueous solutions of perfluoroalkyl carboxylates[3−6] has been reported in the literature since 1987, the first structural investigation of the $n_2$ micellar solutions has been only recently reported.[1−2] PFPE carboxylic salts form a wide range of self-association structures in water from liquid crystals[7−9] to microemulsions[10−14] to micellar solutions.[9,15−19] The micellization and phase behavior in water of the ammonium and sodium salts used in refs 1 and 2 and in this work have been previously reported in refs 13 and 15−17.

In previous studies[1,2] we reported that, in the surfactant concentration range 0.05−0.12 M, at 28 °C, ammonium and potassium micelles are spherical in shape with inner core radius of 15 Å and interfacial layer thickness of 4.0 Å. At 0.2 M concentration, both counterions provided prolate ellipsoidal micelles, with axial ratio 2, and minor axis of 13 Å at 28 and 40 °C: at 80 °C only the ammonium micelles rearrange into spherical micelles of ~15 Å core radius. For both counterions, the micellar size distribution is extremely narrow and the average aggregation numbers, as well as the surface charge, are found to slightly differ for the two counterions upon variation of concentration and temperature, with fractional ionizations spanning from 0.3 to 0.5. By conductometry, Kallay et al.[15] investigated the ammonium $n_2$ micellar solutions, finding, at 25 °C, a micellar contact potential of 59 meV and fractional ionization of 0.36 in good agreement with the value 63 meV (recalculated at 25 °C) and 0.44, both of our previous work.[2]

This paper is a continuation of previous works[1,2] on ammonium and potassium $n_2$ micellar solutions. Lithium, sodium, cesium and diethanol ammonium $n_2$ micellar solutions are studied to have better insight on the micellar microstructural changes as a function of the counterions. As in previous works,[1,2] SANS spectra have been analyzed by a two-shell model for the micellar form factor and a screened Coulombic plus steric repulsion potential for the structure factor. The results from the $n_2$ micellar solutions are also compared with the results of

* Corresponding author.
† University of Florence and I.N.F.M.
‡ I.N.F.M. CRS-SOFT, Universitá Roma "La Sapienza".
§ University of Messina and I.N.F.M.
|| Solvay Solexis.
⊥ University of Florence and C.S.G.I.
▽ CEA-CNRS Saclay.

10.1021/jp0405815 CCC: $30.25 
Published on Web 04/02/2005

**TABLE 1: Volume ($V$), Scattering Length (s.l.) and Scattering Length Density ($\rho$) of the Counterions**

| | $V$ (Å$^3$) | s.l. ($10^{-12}$ cm) | $\rho$ ($10^{10}$ cm$^{-2}$) |
|---|---|---|---|
| $Li^+$ | 1.376 | −0.190 | −13.81 |
| $Na^+$ | 4.445 | 0.363 | 8.166 |
| $Cs^+$ | 20.58 | 0.542 | 2.634 |
| $H_2NR_2^+$ | 160 | 0.268 | 0.1675 |

hydrogenated alkali micellar solutions and perfluoroalkyl carboxylates micellar solutions.

### Modeling Micelles

SANS scattered neutron cross section per unit volume of the sample was measured vs the momentum transfer $Q$. The micellar solution is assumed to be composed of surfactant molecules at the critical micellar concentration, cmc, and micelles with an average surfactant aggregation number $N$, with an effective micellar charge $Q^*$.

To define the normalized particle form factor $P(Q)$, the micelle has been modeled as a two-shell particle, formed of a core containing the surfactant tails and an interfacial layer containing the $CO_2^-$ surfactant polar headgroups, some counterions $X^+$, and hydration water molecules. In refs 1 and 2 a net separation between the fluorinated and the hydrogenated region of the micelle was assumed on the basis of the high hydrophobicity of fluorinated molecules.[20] For the particle form factor $P(Q)$ we use spherical or ellipsoidal shapes, as detailed in ref 2. The core radius of the spheres $R_c$, the core short and long axes $b$ and $a$, respectively, and the shell thickness $t$ are sufficient to define the micelles size and shape.

The interparticle structure factor $S(Q)$ is the result of steric repulsion and screened Coulombic repulsion between micelles[21−24] and it has been calculated by assuming an analytical solution for the multicomponent ionic liquid with a mean spherical approximation (MMSA).[25−27] The multicomponent system was reduced to a generalized one-component macroion (GOCM) system.[28,29] A detailed description of the theoretical framework is reported in refs 30−32. According to theory, the total neutron cross section per unit volume of the sample can be written[32]

$$I(Q) = C_M N\left(\sum_i b_i - V_m \rho_S\right)^2 P(Q)\, S(Q) + I_{back}$$

where $C_M$ is the number density of the surfactant molecules in micelles ($C_M = C - cmc$, with C surfactant concentration and cmc critical micellar concentration), $N$ is the average surfactant aggregation number of the micelle (already defined), $\Sigma_i b_i$ is the total scattering length of all the atoms in the surfactant molecule, $V_m$ is the surfactant molecule volume, or monomer volume, and $\rho_s$ is the scattering density of the solvent, i.e., the $H_2O$ scattering length divided by the $H_2O$ molecule volume. The spectrum background, $I_{back}$, is due to the incoherent contribution of the atoms. The term $\Sigma_i b_i - V_m \rho_S$ represents the contrast, i.e., the difference between the scattering length of the dry surfactant molecule and the solvent molecules of equivalent volume. The scattering length density of the two parts of a micelle, $\rho_1$ (that of the hydrophobic core) and $\rho_2$ (that of the shell) have been evaluated as reported in ref 2. The values of the volume and scattering length for the different counterions of this paper are reported in Table 1. The volumes of lithium, sodium and cesium dry counterions are taken from ref 33, and that of the diethanol ammonium counterion has been calculated by assuming the density of diethanolamine ($\rho = 1.09$ g/cm$^3$ at 20 °C). A detailed description of the spherical and ellipsoidal form factors $P(Q)$, of the interparticle structure factor $S(Q)$ and the interaction potential $U$ that have been used to fit the data is reported in ref 2. The macroion structure factor was calculated using a revised version of Hayter−Penfold's Fortran package.[21]

### Materials

The salts of lithium ($Li^+$), sodium ($Na^+$), cesium ($Cs^+$) and diethanol ammonium ($H_2NR_2^+$ with R = $(CH_2CH_2OH)_2^+$) of the carboxylic acid $Cl(C_3F_6O)_2CF_2COOH$ (PFPE type with two perfluoroisopropoxy units in the hydrophobic chain) were provided by Solvay Solexis, Milan, Italy, with a purity of 99.8%.

The molecular weight of the acid obtained by titration and NMR agreed within 5% experimental error with the calculated value (MW = 462). The dry salts, prepared by neutralizing the acid with a stoichiometric amount of the corresponding hydroxide, were free of acid and inorganic impurities within analytical sensitivities. All the solutions were prepared using Milli-Q water. The basic information of the phase behavior in water and micellization of the $Na^+$, $K^+$, $NH_4^+$ salts in water are available in ref 13, including cmc and concentration threshold for liquid crystal formation at room temperature. Qualitatively similar behavior has been detected for the other salts of the present work. The liquid crystal concentration threshold, detected by visual observation and optical microscopy in polarized light, is found for the alkali metals to follow the trend of counterion hydration, $Li^+ > Na^+ > Cs^+$. The onset of liquid crystal formation spans from about 50 wt % to 45 wt % and 17 wt for $Li^+$, $Na^+$ and $Cs^+$, respectively, whereas the diethanol ammonium salt has a concentration threshold of about 22%, close to the 25% of the ammonium surfactant.[2] Because the surfactant concentrations studied in this work are well below these limits, all the micellar solutions were macroscopic single isotropic phases and were individually checked for invariance upon aging or centrifugation. Critical micellar concentrations were $2.6 \times 10^{-2}$ M, $2.0 \times 10^{-2}$ M and $1.9 \times 10^{-2}$ M for $Li^+$, $Na^+$, and $Cs^+$, respectively, and $3.5 \times 10^{-2}$ M for the diethanol ammonium salt at 28 °C. Throughout the paper we used the cmc value obtained at 28 °C because cmc variation with temperature is negligible.

### Method

SANS experiments were performed at the PAXE spectrometer (Lab. Léon Brillouin, Saclay) with a sample−detector distance of 2.56 m and 5 Å incident neutron wavelength with a wavelength spread of 10%. Collimation was achieved by two slits of 12 and 7 mm diameter, placed 2.5 m far apart. Samples were contained in flat quartz cells of 1 mm thickness, and measured at 28 40, and 67 °C with a thermal stability of ±0.1 °C. The two-dimensional intensity distributions were corrected for the background and the empty cell contributions and then normalized to absolute intensity by a direct measurement of the intensity of the incident neutron beam.[30,34] By integrating the normalized two-dimensional intensity distribution with respect to the azimuthal angle, one-dimensional scattering intensity distributions $I(Q)$ in the unit of a differential cross section per unit volume (cm$^{-1}$) were obtained.

### Results

The experimental spectra at 28, 40, and 67 °C are shown in Figures 1−3 for ionic micellar solutions with lithium, sodium and cesium counterions, respectively, at 0.2 M surfactant concentration. For the three series of samples, the presence of the structural peak suggests that significant interactions between micelles occur and an increase of temperature from 28 to 67

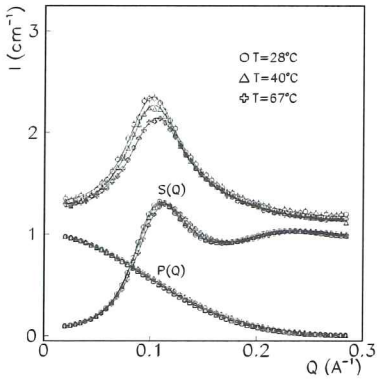


**Figure 1.** Experimental scattered intensity $I$ (cm$^{-1}$) vs $Q$ (Å$^{-1}$) of lithium counterion micellar solutions at 0.2235 M concentration and temperatures of 28 °C (circles), 40 °C (triangles) and 67 °C (crosses). Continuous lines are the fitted curves. The corresponding normalized form $P(Q)$ and structure $S(Q)$ factors are reported in the bottom part of the figure for each sample (symbols as above) connected by dashed and continuous lines, respectively. The vertical scale of the normalized form and structure factors is dimensionless.

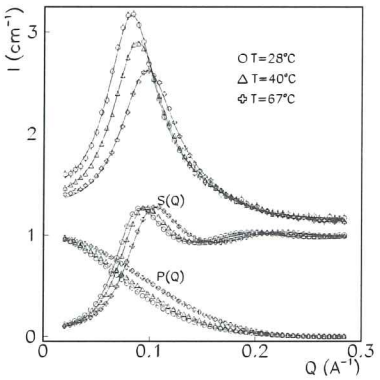


**Figure 3.** Experimental scattered intensity $I$ (cm$^{-1}$) vs $Q$ (Å$^{-1}$) of micellar solutions with cesium counterion at 0.2205 M concentration and temperatures of 28 °C (circles), 40 °C (triangles) and 67 °C (crosses). Continuous lines are the fitted curves. The corresponding normalized form $P(Q)$ and structure $S(Q)$ factors are reported in the bottom part of the figure for each sample (symbols as above) connected by dashed and continuous lines, respectively. The vertical scale of the normalized form and structure factors is dimensionless.

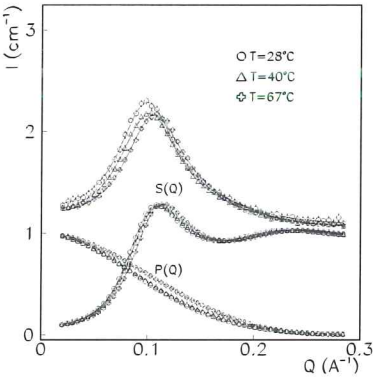


**Figure 2.** Experimental scattered intensity $I$ (cm$^{-1}$) vs $Q$ (Å$^{-1}$) of micellar solutions with sodium counterion at 0.2161 M concentration and temperatures of 28 °C (circles), 40 °C (triangles) and 67 °C (crosses). Continuous lines are the fitted curves. The corresponding normalized form $P(Q)$ and structure $S(Q)$ factors are reported in the bottom part of the figure for each sample (symbols as above) connected by dashed and continuous lines, respectively. The vertical scale of the normalized form and structure factors is dimensionless.

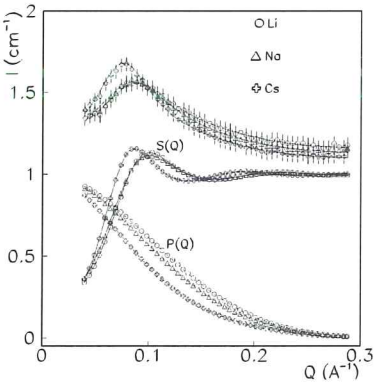


**Figure 4.** Experimental scattered intensity $I$ (cm$^{-1}$) vs $Q$ (Å$^{-1}$) of micellar solutions at 28 °C with lithium, sodium and cesium counterions at concentrations of 0.1092 M (circles), 0.1055 M (triangles) and 0.1045 (crosses), respectively. Continuous lines are the fitted curves. The corresponding normalized form $P(Q)$ and structure $S(Q)$ factors are reported in the bottom part of the figure for each sample (symbols as above) connected by dashed and continuous lines, respectively. The vertical scale of the normalized form and structure factors is dimensionless.

°C produces a decrease of the peak intensity and a shift of the peak position toward larger $Q$ values. This trend is more pronounced for cesium micellar solutions. Less pronounced peaks are shown in Figure 4, where the experimental spectra are reported for lithium, sodium and cesium counterions at a constant temperature of 28 °C and 0.1 M concentration. Figure 5 reports SANS spectra of ionic micellar solutions with diethanol ammonium counterion at 0.1 and 0.2 M surfactant concentration and 28 °C. In Figures 1−5, the fitted curves according to the theoretical models (continuous lines) and the form and structure factors (dashed and continuous lines, respectively) are reported for each sample.

In Table 2 are reported the free fitting parameters evaluated for each sample by fitting the experimental data to the eq 1. There are five parameters for the spherical model ($Q^*$, $N$, $R_c$, $t$, and polydispersity) and four for the ellipsoidal model ($Q^*$, $N$, $b$, t). $b$ and $R_c$ are reported in the same column of Table 2; when the $a/b$ axial ratio is given, the value of the column is $b$; when the axial ratio is not given, the micelles are spherical and the value of the column is $R_c$. For all the samples, the quality of the fit was deduced by the $\chi^2$ values, which is close to 1. From the results of Table 2, the micelles show an ellipsoidal shape, except sodium and cesium micelles at 67 °C, which are spherical. In fact, for the latter samples, the best fit of the spherical model leads to $\chi^2$ values smaller than the best fit of the ellipsoidal model. The calculated polydispersity of the spherical micelles is less than 10% and corresponds to the intrinsic polydispersity of the measurements in the experimental conditions used. Thus we consider the micelles monodispersed.

In addition to the free fitting parameters, for all the samples studied, Table 2 reports some other parameters calculated by the previous ones, i.e., the fractional ionization $\alpha = Q^*/N$ that represents the number of free counterions surrounding each micelle (i.e., the number of unscreened surfactant headgroups of a micelle), the axial ratio $a/b$ (where the long axis is calculated by the relationship $a = 3NV_{tail}/4\pi b^2$), the number of interfacial water molecules for surfactant molecule, $N_S$ (or hydration number per surfactant molecule), the diameter $D$ of spherical micelles or, in the case of ellipsoidal micelles, the diameter of a sphere with the same volume, the Debye length $l_D$, the contact potential $U_1$ and the volume fraction of micelles $\eta$. In Table 3, the inner (core−shell) and outer (micelle−solvent) surface areas

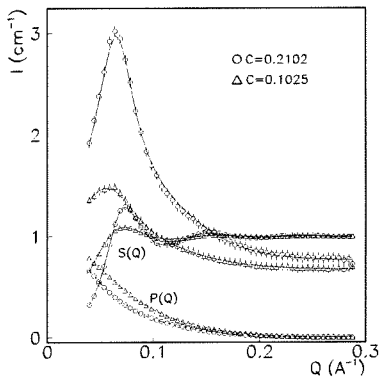


**Figure 5.** Experimental scattered intensity $I$ ($cm^{-1}$) vs $Q$ ($Å^{-1}$) of micellar solutions with diethanol ammonium counterion at 28 °C with concentrations of 0.2102 M (circles) and 0.1025 M (triangles). Continuous lines are the fitted curves. The corresponding normalized form $P(Q)$ and structure $S(Q)$ factors are reported in the bottom part of the figure for each sample (symbols as above) connected by dashed and continuous lines, respectively. The vertical scale of the normalized form and structure factors is dimensionless.

per polar head are calculated from the geometrical parameters ($b$, or $R_c$, $a$, and $t$) and $N$ of Table 2. $\Sigma_{inner}$ is the surfactant area per polar head. The accuracy of $Q^*$ and $N$ is 3%; thus α is known with 6% accuracy. The thickness $t$ is known with 10%, core radius $R_c$, short axis $b$ and diameter $D$ with 2%, axial ratio $a/b$ with 4%, and $\Sigma_{inner}$ with 5% accuracy for ellipsoids and 7% for spheres. A lower accuracy was achieved at $C = 0.1$ M because of the small coherent part of the spectrum.

The results of Tables 2 and 3 evidence similarities and differences between the lithium, sodium and cesium micelles. The micelle's shell thickness, 4.0 Å, for the three counterions, is not affected by concentration and temperature. At 28 °C for both 0.1 and 0.2 M surfactant concentrations, the sodium, lithium and cesium micelles are prolate ellipsoidal particles with an axial ratio that increases from 1.6 to 2.7 as the counterion volume increases. The short axis is $b \sim 13$ Å for all the micelles. The lithium micelles show a very stable ellipsoidal form factor in the concentration and temperature range studied, whereas the cesium and sodium micelles are ellipsoidal at 28 and 40 °C with axial ratio 2 or more, and at 67 °C they are spheres of core radius ~15 Å. The area per polar head (Table 3), at 28 °C and $C = 0.2$ M, is 75 ± 4 $Å^2$ for lithium and sodium micelles and 66 ± 3 $Å^2$ for cesium micelles, i.e., smaller for the larger counterion in the limit of the experimental errors. At $C = 0.2$ M, the increase of temperature to 67 °C increases the area per polar head for lithium and sodium micelles; a less pronounced increase is observed for cesium micelles in the limit of the experimental errors. The decrease of concentration from 0.2 to 0.1 M at 28 °C leads to significant larger area per polar head.

For the three counterions, at 28 °C (Table 2) the average aggregation number, $N$, significantly increases with increasing concentration and decreases with increasing temperature at $C = 0.2$ M. The micellar charge also increases with concentration at 28 °C and it is independent of temperature at $C = 0.2$ M. Thus, the fractional ionization α is stable, 0.50, for lithium micelles in the limit of the experimental errors, whereas for sodium micelles it is 0.40 vs concentration and increases vs temperature from 0.40 to 0.55 at $C = 0.2$ M. For cesium micelles α decreases with increasing concentration at 28 °C from 0.40 to 0.30 and increases with increasing temperature at $C = 0.2$ M from 0.30 to 0.40. These findings show that cesium micelles are less charged than lithium and sodium micelles; i.e., more counterions are bound to the micellar polar heads. Table 2 shows also that the number of water molecules for surfactant molecule of lithium and sodium micelles is 13, whereas for cesium micelles is 10.

The volume fraction of micelles, $\eta$, is in agreement with the micellized surfactant concentration for all the samples of this work.

The decrease of concentration at 28 °C, for lithium and sodium micelles, leads to a decrease of the contact potential and an increase of the Debye length, whereas for cesium micelles both contact potential and Debye length increase. At $C = 0.2$ M, the increase of temperature does not affect significantly both the contact potential and Debye length. This last result is due to the joint increase of temperature and fractional ionization. In fact, $l_D^2$ is proportional to temperature and to $1/\alpha$.[35]

The micelles of diethanol ammonium salt at 28 °C (see Table 2) are ellipsoidal with short axis $b = 14$ Å for both concentrations and shell thickness $t = 5.1$ Å, higher than the value (4.0 Å) of the previous alkali micelles likely because the diethanol ammonium counterion volume (160 $Å^3$) is larger than the polar head volume, 35 $Å^3$.[2] The ellipsoidal axial ratio is 3 at $C = 0.1$ M and 4 at $C = 0.2$ M, indicating that the increase of the dry counterion volume leads to more ellipsoidal shapes.

The effective charge and the average aggregation number are also higher if compared to the previous alkali micelles but lead to lower ionization degrees, 0.26, because of the very large $N$ values. A larger number of counterions is bound to the micellar polar head and the number of water molecules per polar head is 9 (lowest value).

Thus, like for cesium micelles, a larger counterion volume and a smaller hydration number for polar head favor counterion binding to the polar heads, micellar growth and lower area per polar head ~70 $Å^2$ (Table 3) for both concentrations. As for lithium and sodium micelles, the concentration decrease at 28 °C leads to a contact potential decrease and Debye length increase.

## Discussion

To have a better insight on the role of counterions and temperature in $n_2$ micellar solutions, it is worthy to compare the above results with those of the potassium and ammonium $n_2$ micelles.[1,2]

The **potassium** micelles at 28 °C are spherical of radius 14 Å at 0.07 and 0.1 M surfactant concentrations whereas they are prolate ellipsoidal at $C = 0.2$ M with axial ratio 2 (similar to lithium and sodium micelles). The core radius $R_c = 14$ Å, the short axis length $b = 12$ Å and the shell thickness $t = 4.1$ Å are independent of temperature in the thermal range 28−80 °C and very similar to the alkali micelles of this work. The area per polar head at 28 °C is 77 $Å^2$ at $C = 0.2$ M (slightly larger at C = 0.1 M) and it increases up to 96 $Å^2$ at 80 °C with a similar trend of the lithium and sodium micelles in the range 28−67 °C.

Charges and average aggregation numbers are also similar to those of alkali micelles of this work and lead to a fractional ionization ~0.44. The number of water molecules for the surfactant polar head is 13, like for lithium and sodium micelles. At 28 °C, the Debye length and the contact potential increase with decreasing concentration, like for cesium micelles, whereas they are constant, at $C = 0.2$ M, vs temperature, like for all the alkali micelles of this work.

In summary, for the alkali micellar solutions the shell thickness (4.0 Å for lithium, sodium, potassium and cesium counterions) is not affected by differences in the concentration

**TABLE 2: SANS Results of $n_2$ PFPE Ionic Micellar Solutions with $Li^+$, $Na^+$, and $Cs^+$ Counterions at Temperatures of 28, 40, and 67 °C and with $H_2NR_2^+$ Counterion at 28 °C[a]**

| $C$ (M) | $Q^*$ | $N$ | t (Å) | $R_c(b)$ (Å) | α | $D$ (Å) | $a/b$ | $N_S$ | $l_D$ (Å) | $U_1$ ($k_BT$) | $\eta$ | $\chi^2$ |
|---|---|---|---|---|---|---|---|---|---|---|---|---|
| | | | | | | $Li^+$ at 28 °C | | | | | | |
| 0.1092 | 14 | 30 | 4.0 | 12 | 0.47 | 36 | 1.6 | 14 | 14 | 7.6 | 0.042 | 1.0 |
| 0.2235 | 21.0 | 40.0 | 4.1 | 13.2 | 0.53 | 39 | 1.6 | 12 | 11 | 10 | 0.093 | 1.0 |
| | | | | | | $Li^+$ at 40 °C | | | | | | |
| 0.2235 | 20.2 | 38.2 | 4.0 | 13.0 | 0.53 | 39 | 1.6 | 12 | 11 | 10 | 0.093 | 1.0 |
| | | | | | | $Li^+$ at 67 °C | | | | | | |
| 0.2235 | 19.0 | 34.9 | 4.0 | 12.6 | 0.54 | 38 | 1.6 | 13 | 12 | 8.5 | 0.095 | 1.0 |
| | | | | | | $Na^+$ at 28 °C | | | | | | |
| 0.1055 | 12 | 32 | 4.0 | 12 | 0.38 | 37 | 1.9 | 14 | 16 | 5.8 | 0.043 | 1.2 |
| 0.2161 | 17.4 | 41.0 | 4.0 | 12.4 | 0.42 | 39 | 2.0 | 12 | 12 | 8.1 | 0.092 | 1.0 |
| | | | | | | $Na^+$ at 40 °C | | | | | | |
| 0.2161 | 16.8 | 38.6 | 4.0 | 12.2 | 0.44 | 39 | 1.9 | 12 | 13 | 7.6 | 0.093 | 1.0 |
| | | | | | | $Na^+$ at 67 °C | | | | | | |
| 0.2161 | 18.0 | 32.0 | 4.0 | 15.0 | 0.56 | 38 | | 14 | 12 | 8.2 | 0.102 | 1.2 |
| | | | | | | $Cs^+$ at 28 °C | | | | | | |
| 0.1045 | 17 | 44 | 4.0 | 12 | 0.39 | 41 | 2.7 | 12 | 16 | 10 | 0.041 | 1.0 |
| 0.2205 | 19.5 | 72.2 | 4.0 | 14.2 | 0.28 | 46 | 2.3 | 9.2 | 14 | 8.5 | 0.086 | 1.0 |
| | | | | | | $Cs^+$ at 40 °C | | | | | | |
| 0.2205 | 19.3 | 60.5 | 4.0 | 14.1 | 0.31 | 44 | 2.0 | 9.7 | 14 | 8.7 | 0.088 | 1.0 |
| | | | | | | $Cs^+$ at 67 °C | | | | | | |
| 0.2205 | 19.0 | 45.0 | 4.0 | 16.0 | 0.42 | 40 | | 11 | 13 | 8.9 | 0.090 | 1.0 |
| | | | | | | $H_2NR_2^+$ at 28 °C | | | | | | |
| 0.1025 | 20 | 85 | 5.0 | 14 | 0.24 | 51 | 3.0 | 8.7 | 15 | 7.7 | 0.033 | 1.0 |
| 0.2102 | 33.0 | 126 | 5.2 | 13.9 | 0.27 | 57 | 4.2 | 8.5 | 13 | 13 | 0.084 | 1.8 |

[a] $C$ is the molar surfactant concentration. $Q^*$ is effective charge, $N$ is average aggregation number, $t$ is micellar shell thickness, $R_c$ is micellar core radius, $b$ is micellar inner minor axis, α is fractional ionization, $D$ is diameter of the equivalent spherical micelle, $a/b$ is axial ratio with $a$ major axis of the micelle, $N_s$ is hydration number, $l_D$ is Debye's length, $U_1$ is potential on the micellar surface, and $\eta$ is volume fraction of the micelles. Reduced $\chi^2$.

**TABLE 3: Inner and Outer Surface per Polar Head Group Calculated from the Results Reported in Table 2**

| $C$ (M) | $\Sigma_{inner}$ (Å$^2$) | $\Sigma_{outer}$ (Å$^2$) |
|---|---|---|
| | $Li^+$ at 28 °C | |
| 0.1092 | 86 | 152 |
| 0.2235 | 75 | 129 |
| | $Li^+$ at 40 °C | |
| 0.2235 | 79 | 136 |
| | $Li^+$ at 67 °C | |
| 0.2235 | 86 | 147 |
| | $Na^+$ at 28 °C | |
| 0.1055 | 93 | 164 |
| 0.2161 | 75 | 134 |
| | $Na^+$ at 40 °C | |
| 0.2161 | 76 | 135 |
| | $Na^+$ at 67 °C | |
| 0.2161 | 88 | 142 |
| | $Cs^+$ at 28 °C | |
| 0.1045 | 92 | 163 |
| 0.2205 | 66 | 109 |
| | $Cs^+$ at 40 °C | |
| 0.2205 | 69 | 114 |
| | $Cs^+$ at 67 °C | |
| 0.2205 | 72 | 112 |
| | $H_2NR_2^+$ at 28 °C | |
| 0.1025 | 71 | 131 |
| 0.2102 | 67 | 125 |

and temperature ranges studied; thus the shell thickness mainly depends on the carboxylate head. The core short axis 13 Å, or the core radius 15 Å, is independent of counterions, meaning that it is mainly determined by the steric and hydrophobic surfactant tail−tail interactions. Micellar charge and average aggregation number depend on concentration, temperature and counterion. At 28 °C, the fractional ionization decreases vs the counterion dry volume (or molecular weight) increase at constant concentration 0.1 and 0.2 M. This implies that the larger counterion, cesium, binds more efficiently to the micellar polar heads. Less charged micelles can grow better because of the reduced repulsion between the polar heads; thus $N$ can increase and higher $a/b$ axial ratios are found. Furthermore, the cesium polar head hydration number is the lowest as the cesium area per polar head. As demonstrated in ref 2 for ammonium and potassium $n_2$ micellar solutions, the micellar growth is dominated by the number density of micelles rather than by the micellar size; in fact, the $Q$ value corresponding to the peak position of the structure factor varies linearly with $((C - \text{cmc})/N)^{-1/3}$. In ref 2 and in this work the average micellar diameter (see Table 2) does not change significantly for each counterion vs concentration or temperature, except when a rod to sphere transition is observed.

The physical origin of the higher binding to the micellar polar heads remains an open question that could be clarified by investigating the dynamics of the micellar interfacial region from the point of view of dipolar interactions of the polar head−counterion and of the bound water, as recently performed by dielectric spectroscopy on sodium dodecyl sulfate micellar solutions.[36]

At $C = 0.2$ M the fractional ionization α is constant vs temperature for the alkali micelles with ellipsoidal geometry. In correspondence to the transition from ellipsoids to spheres, at 67 °C for sodium and cesium micelles, α increases.

In ref 9 the surfactant areas per polar head evaluated by surface tension measurements close to the cmc, 77 Å$^2$ for sodium, 71 Å$^2$ for potassium and 74 Å$^2$ for ammonium PFPE micellar solutions, are in good agreement with the values of

the most concentrated micelles of ref 2 and of this work, in the limit of the experimental errors. Furthermore, above the cmc, the counterion binding in sodium micelles is larger than that of potassium and ammonium micelles such as in this paper at $C = 0.2$ M. An ellipsoidal short axis $b = 10.6$ Å and an axial ratio $a/b = 4$ for sodium $n_2$ PFPE micelles at 20 wt % surfactant concentration were found by SAXS in ref 19. These values agree with the values of the sodium micelles of this work. In fact, they indicate that, increasing the surfactant concentration up to 0.4 and 0.8 M, the micelles grow with the same prolate ellipsoidal geometry. The increase of $N$ with surfactant concentration is also evidenced by the fluorescence probe study for sodium and ammonium $n_2$ PFPE micellar solutions,[16,17] where the $N$ values are larger for ammonium than for sodium micelles, as found by SANS for sodium micelles in this paper and for ammonium micelles in ref 2. The counterion binding of ammonium and sodium micelles was also evaluated in refs 16 and 17, leading to lower values for sodium micelles, as also found, in the case of ellipsoidal shape, by SANS in this paper for sodium and in ref 2 for ammonium micelles.

With the aim of understanding if the observed trends are due to the presence of fluorine atoms in the surfactant molecules, we compare our results on alkali micelles with those on hydrogenated dodecyl sulfate aqueous micellar solutions with lithium,[26,37−39] sodium[26,31,38,39] and cesium counterions.[31,39] The geometrical parameters, the surface charges and the average aggregation numbers of the hydrogenated micelles are obviously different in comparison with the micelles of refs 1 and 2 and of this work. However, all the hydrogenated micelles are prolate ellipsoidal with similar or lower axial ratios and lower fractional ionizations and the increase of counterion volume gives a fractional ionization decrease and an axial ratio increase as also found in our case. The mechanism of micellar growth induced by higher binding of the larger counterion seems to be general. In fact, also in hydrogenated cationic surfactant cetyltrimethylammonium bromide (CTABr) or chlorine (CTACl) micellar solutions the same mechanism occurs.[40]

The comparison of the **diethanol ammonium** micellar solutions with the ammonium micellar solutions studied in refs 1 and 2 that differ for the counterion volume show that the ammonium micelles at 28 °C are spherical at $C = 0.05$ M and $C = 0.1$ M and ellipsoidal at $C = 0.2$ M; on the contrary, the diethanol ammonium micelles are ellipsoidal at $C = 0.1$ M and $C = 0.2$ M with higher $a/b$ axial ratios. The interfacial layer of ammonium micelles is 3.8 Å like for the alkali micelles of this work (in the limit of the experimental errors) and 5.1 Å for the diethanol ammonium micelles.

This finding suggests that, when the counterion volume is very large, the shell thickness depends on the counterion also. The diethanol ammonium micellar core short axis $b = 14$ Å for both ammonium and diethanol ammonium micelles, is slightly larger than that of the alkali micelles of this work at 28 °C; thus the hydrophobic tails attract each other a bit more than in the alkali micelles, leading to larger micellar aggregation numbers that arrange into more ellipsoidal particles at similar surfactant concentration. This comparison confirms that the inner core dimension is mainly due to the surfactant steric tail−tail interaction and the interfacial layer is mainly due to the carboxylate polar head, influenced by the counterion dimension in the case of the bulky diethanol ammonium counterion. The axial ratio of ammonium micelles $a/b \sim 2.4$ is smaller, confirming that, also in this case, the bigger counterion favors ellipticity. Slightly smaller charges and very smaller average aggregation numbers lead to ionization degrees higher for ammonium micelles (0.40) than for diethanol ammonium micelles as for the alkali micelles.

The contact potential and Debye length are similar for both micellar solutions being due to a similar charge distribution on the micellar surface. The area per polar head of ammonium micelles[2] is ~70 Å$^2$ at $C \sim 0.2$ M, very similar to the value of diethanol ammonium micelles.

It is interesting to compare the results of this paper with those of perfluoroctane (PFO) micellar solutions because the PFO is a fluorinated surfactant with a tail length similar to that of the $n_2$ surfactant. The comparison with lithium, sodium and cesium PFO micellar solutions, with surfactant concentrations similar to ours, shows very different micellar shapes. In fact, by SANS, lithium and sodium micelles were found to be spherical[4,41] and cesium micelles were oblate ellipsoids.[5] These differences could be explained by the presence of oxygen and of the lateral chain in the PFPE tail of the $n_2$ surfactant of this work.

**Acknowledgment.** We thank S. Fontana and C. Tonelli for the thorough purification of the materials. Acknowledgments are due to EC for support via the TMR-LFS Program (Contract N. HPRI-1999-CT-00032) and to MURST (PRIN 2003), INFM and CSGI for financial support.

## References and Notes

(1) Gambi, C. M. C.; Giordano, R.; Chittofrati, A.; Pieri, R.; Baglioni, P.; Teixeira, J. *Appl. Phys. A* **2002**, *74* [Suppl.], 5436.
(2) Gambi, C. M. C.; Giordano, R.; Chittofrati, A.; Pieri, R.; Baglioni, P.; Teixeira, J. *Phys. Chem. A* **2003**, *107*, 11558.
(3) Burkitt, S. J.; Ottewill, R. H.; Hayter, J. B.; Ingram B. T. *Colloid Polym. Sci.* **1987**, *265*, 619.
(4) Berr, S. S.; Jones R. R. M. *J. Phys. Chem.* **1989**, *93*, 2555.
(5) Iijima, H.; Kato, T.; Yoshida, H.; Imai, M. *J. Phys. Chem. B* **1998**, *102*, 990.
(6) Iampietro, D. J.; Kaler, E. W. *Langmuir* **1999**, *15*, 8590−8601.
(7) Wurtz, J.; Meyer, J.; Hoffmann, H. *Phys. Chem. Chem. Phys.* **2001**, *3*, 3132.
(8) Caboi, F.; Chittofrati, A.; Monduzzi, M.; Morioni, C. *Langmuir* **1996**, *12*, 6022−6027.
(9) Caboi, F.; Chittofrati, A.; Lazzari, P.; Monduzzi, M. *Colloids Surf. A: Physicochem. Eng. Aspects* **1999**, *160*, 47.
(10) Baglioni, P.; Gambi, C. M. C.; Giordano, R.; Senatra, D. *J. Mol. Struct.* **1996**, *383*, 165−169.
(11) Baglioni, P.; Gambi, C. M. C.; Giordano, R. *Physica B* **1997**, *234−236*, 295−296.
(12) Monduzzi, M.; Knacksted, M. A.; Ninham, B. W. *J. Phys. Chem* **1995**, *99*, 17772.
(13) Chittofrati, A.; Pieri, R.; D'Aprile, F.; Lenti, D.; Maccone, P.; Visca, M. *Prog. Colloid Polym. Sci.* **2004**, *123*, 23.
(14) Mele, S.; Chittofrati, A.; Ninham, B. W.; Monduzzi, M. *J. Phys. Chem. B* **2004**, *108*, 8201.
(15) Kallay, N.; Tomii, V.; Hrust, V.; Pieri, R.; Chittofrati, A. *Colloid Surf. A* **2002**, *222*, 95.
(16) Sulak, K.; Szajdzinska-Pietek, E. In *Proceedings of the Conference "Surfactants and Dispersed Systems in Theory and Practice"*, Soruz, Polanica Zdroj, May 20−23; Wilk, K. A., Ed.; Oficina Wydawnicza Politechniki Wroclawskiej: Wroclaw, Poland, 2003.
(17) Sulak, K.; Wolszczak, M.; Chittofrati, A.; Szajdzinska-Pietek, E. *J. Phys. Chem. B* **2005**, *109*, 799.
(18) Mele, S.; Murgia, S.; Monduzzi, M. *J. Fluorine Chem.* **2004**, *125*, 261−269.
(19) Mele, S.; Ninham, B. W.; Monduzzi, M. *J. Phys. Chem. B* **2004**, *108*, 17751.
(20) Kissa, E. In *Fluorinated Surfactants*; Surfactant Science Series 50; Marcel Dekker: New York, 1994.
(21) Hayter, J. B.; Penfold, J. J. *J. Mol. Phys.* **1981**, *42*, 109.
(22) Hayter, J. B.; Penfold, J. J. *J. Chem. Soc., Faraday Trans.* **1981**, *77*, 1851.
(23) Snook, I. K.; Hayter, J. B. *Langmuir* **1992**, *8*, 2880−2884.
(24) Hunter, R. J. In *Foundation of Colloid Science*; Oxford Science Publications: Clarendon Press: Oxford, England; Oxford University Press: New York, 1989; Vol. 2, Chapter 14.
(25) Hansen, J. P.; Hayter, J. B. *Mol. Phys.* **1982**, *46*, 651−656.
(26) Sheu, E. Y.; Wu, C. F.; Chen, S.-H.; Blum, L. *Phys. Rev. A* **1985**, *32*, 3807.

(27) Senatore, G. In *Structure and Dynamics of Strongly Interacting Colloids and Supramolecular Aggregates in Solutions*; Chen, S.-H., Huang, J. S., Tartaglia, P., Eds.; Kluwer Academic Publisher: Dordrecht, The Netherlands, 1992; pp 175−189.

(28) Chen, S.-H.; Sheu, E. Y. In *Micellar Solutions and Microemulsions. Structure, Dynamics, and Statistical Thermodynamics*; Chen, S. H., Rajagopalan, R., Eds.; Springer−Verlag: New York, 1990; pp 3−28.

(29) Chen, S. H.; Sheu, E. Y.; Kalus, J.; Hoffmann, H. *J. Appl. Crystallogr.* **1988**, *21*, 751.

(30) Liu, Y. C.; Baglioni, P.; Teixeira, J.; Chen, S.-H. *J. Phys. Chem.* **1994**, *98*, 10208.

(31) Liu, Y. C.; Ku, C. K.; Lo Nostro, P.; Chen, S.-H. *Phys. Rev. E* **1995**, *51*, 4598.

(32) Sheu, E. Y.; Chen, S.-H.; Huang, J. S. *J. Phys Chem.* **1987**, *91*, 1535.

(33) Yizhak, Marcus. In *Ion Properties*; Marcel Dekker: New York, 1997; p 46.

(34) Teixeira, J. In *Structure and Dynamics of Strongly Interacting Colloids and Supramolecular Aggregates in Solutions*; Chen, S.-H., Huang, J. S., Tartaglia, P., Eds.; Kluwer Academic Publisher: Dordrecht, The Nertherlands, 1992; pp 635−658.

(35) Hunter R. J. In *Foundation of Colloid Science*; Oxford Science Publications: Clarendon Press: Oxford University Press: New York, 1987; Vol. I, p 332.

(36) Lanzi, Leandro; Carla' M.; Gambi C. M. C.; Lanzi, L. In *The Physics of Complex Systems - New Advances and Perspectives*; Vol. 155, Proceedings of the International School of Physics "Enrico Fermi"−Course CLV; Mallamace, F., Stanley, H. E., Eds.; IOS Press: Amsterdam 2004; p 507 and work in progress.

(37) Bendedouch, D.; Chen, S.-H.; Koehler, W. C. *J. Phys. Chem.* **1983**, *87*, 2621.

(38) Baglioni, P.; Rivara-Minten, E.; Kevan L. *J. Phys. Chem.* **1988**, *92*, 4726−4730.

(39) Liu, Y. C.; Chen, S.-H.; Itri, R. *J. Phys.: Condens. Matter* **1996**, *8*, A169.

(40) Aswal, V. K.; Goyal, P. S. *Chem. Phys. Lett.* **2003**, *368*, 59−65.

(41) Hoffmann, H.; Kalus J.; Thurn, H. *Colloid Polym. Sci.* **1983**, *261*, 1043.